Oxidation of carbon monoxide and deuterium on a Pd(100) film

H. Fornander, L.-G. Ekedahl and H. Dannetun

Department of Physics and Measurement Technology, Linköping University, SE-581 83 Linköping, Sweden

Received 4 February 1999; accepted 8 April 1999

For Pd/MgO(100) pre-exposed to oxygen, the catalytic oxidation of CO and D_2, respectively, has been studied in the temperature range 100–300 °C. At temperatures $\geqslant$200 °C, the CO_2 desorption rate is independent of oxygen coverage, θ_O, and the reactive sticking coefficient for CO is close to unity. The D_2O desorption rate is strongly dependent on θ_O. D_2 adsorption is blocked by adsorbed oxygen and the maximum D_2O desorption rate is reached when almost all oxygen has been consumed ($\theta_O < 0.03$). The formation of an oxygen c(2 × 2) structure, coexisting with the initial p(2 × 2) phase, is reflected in the oxidation rates.

Keywords: thin films, palladium, magnesium oxide, catalysis

1. Introduction

The practical importance of understanding the reaction kinetics of catalytic reactions on transition metal surfaces cannot be exaggerated. Even though numerous studies have been reported during the years, many questions remain to be answered, even for fairly simple reactions such as the CO and H_2 oxidations.

The work reported here is part of a study of simple catalytic reactions on Pd films, with varying film thicknesses, supported on (100), (111) and (110) single-crystalline MgO. The ambition has been to investigate the relation between catalyst structure and catalyst performance. In this communication we discuss the oxidation of carbon monoxide and hydrogen (deuterium) on a 200 nm Pd film grown on MgO(100). The reason for studying both reactions is that they display very different reaction behaviors and may therefore supply complementary information. Comparative studies of the same reactions have also been performed on 200 nm Pd films grown on MgO(111) and (110), respectively [1] and on model catalysts where Pd films with nominal thicknesses of 1.5, 4 and 20 nm were supported on MgO(100) [2]. The growth and the structural characterization of the Pd/MgO catalysts have been described elsewhere [3,4].

The results presented here origin from titration experiments where the Pd(100) surface has been precovered with oxygen prior to being exposed to hydrogen or CO. Oxygen adsorption on Pd(100) has been extensively studied [5–9] and it is well known that oxygen adsorbs in several different phases on Pd(100). At room temperature, oxygen initially adsorbs in islands forming a p(2×2) phase with a saturation coverage of 1/4 a monolayer. (We define $\theta_O = 1$ monolayer as a coverage with one oxygen atom per Pd surface atom.) After the p(2×2) sites have been filled, oxygen continues to adsorb dissociatively, but at a much slower rate, into the more dense c(2 × 2) phase, for $0.25 < \theta_O < 0.5$. Simmons et al. [5] for instance report that it takes a 2 L (1 L = 1×10^{-6} Torr s) exposure to create a full p(2 × 2) phase at room temperature, whereas a 180 L exposure is needed to create a complete c(2×2) phase. At elevated temperatures the two phases can coexist [5,6] and the c(2 × 2) structure has been observed for coverages below 0.25 [10].

The oxidation of CO on transition metal surfaces has been extensively studied during the years. Ertl and coworkers [11–13] have, e.g., shown that the oxidation of CO on Pd(100), (111) and (110) single crystals as well as on polycrystalline wires follows a Langmuir–Hinshelwood reaction mechanism, i.e., both oxygen and carbon monoxide need to adsorb on the surface before forming CO_2. They furthermore conclude that at steady state the reaction is structure insensitive. Goschnick et al. [14] do, however, state that there are differences in the activation energy and in the pre-exponential in the oxidation reaction rate between the (110) and (111) Pd surfaces, but these effects compensate each other and the overall reaction rates for the two surfaces become the same. Our studies of the transient, isothermal CO_2 production on oxygen pre-exposed (100), (111) and (110) Pd surfaces suggest that there are indeed structure-related differences [1].

Hydrogen oxidation on Pd, which also has been concluded to obey a Langmuir–Hinshelwood reaction mechanism [15], is a system less studied than CO. The two reactions display very different behavior, which is not surprising, considering, e.g., that hydrogen adsorbs dissociatively while CO does not and whereas CO adsorbs at on-top or at bridge positions, hydrogen adsorbs at the same hollow sites as oxygen does.

In our laboratory, studies have been performed on the catalytic oxidation of CO and H_2 on both continuous and discontinuous Pd films grown on SiO_2. In the case of CO and H_2 oxidation on continuous polycrystalline Pd films, the surface reaction kinetics have been modeled to show a very good agreement with experimental data [16–18]. In those studies both CO_2 and H_2O formation rates showed

an oxygen coverage dependency, while in the results presented here for the Pd(100) surface the CO_2 formation rate is almost unaffected by adsorbed oxygen, at least at temperatures above 200 °C. A zero-order oxygen dependency was also reported by Ertl et al. [12] from studies on Pd(111), while our studies on Pd/MgO(111) reveal a slight oxygen coverage dependence [1]. Our water desorption studies on Pd(100), furthermore, show a much more effective inhibition of hydrogen dissociation by oxygen than observed in our previous studies of the SiO_2-supported polycrystalline Pd films.

2. Experimental

The Pd film was grown (as described in [3]) in a separate vacuum chamber, by electron-beam evaporation on a commercial, polished MgO(100) wafer, held at 300 °C. The background pressure in the chamber prior to growth was $<2 \times 10^{-8}$ Torr. The growth rate was kept around 0.1 nm s^{-1}, as monitored using a quartz microbalance. The size of the deposited film was 7×8 mm^2. As determined by AFM, the produced film was flat and continuous with atomic steps.

The sample was loaded in the experimental UHV chamber (where the titration experiments were carried out) via a load-lock system. A few hours after sample loading, the chamber base pressure was of the order of 1×10^{-10} Torr. The pressure was measured with two pressure gauges, a nude hot cathode ionization gauge and a cold cathode Penning gauge. All pressures and exposures given in the paper have been calculated from the hot cathode readings by dividing with the sensitivity factors tabulated by Nakao [19], i.e., 0.87 for O_2, 1.0 for CO, 0.40 for D_2, 0.44 for H_2 and 1.4 for Ar. From earlier experience, and from comparisons between calculated and experimental reaction rate data, we estimate the gauge corrected pressure to be accurate within 10% [16,17].

The UHV chamber is equipped with two quadrupole mass spectrometers. One is placed in front of, and close to, the sample for detection of desorbing products. The detection limit for desorbing water molecules is better than 1×10^{11} molec./cm^2 s, i.e., about 10^{-4} monolayers per second. The second mass spectrometer is placed far, and out of sight, from the sample and controls the background partial pressure of the admitted and residual gases.

The sample was cleaned by alternating H_2 and O_2 exposures at 300 °C. This is a method which is known to produce a clean Pd surface [17,20]. The effect of oxygen/hydrogen exposures on the surface potential was followed with a Kelvin probe and was used to determine when the surface was clean. Furthermore, the electronic structure of the valence band, and thereby also the cleanliness, was checked by ultraviolet photoelectron spectroscopy, utilizing He II resonance radiation. After the oxidation measurements the roughness of the sample surface was investigated by atomic force microscopy using a Nanoscope IIIa from Digital Instruments running in Tapping Mode.

Different oxygen pre-exposures, 0.2–115 L, were produced by exposing the sample to an oxygen pressure of 2.3×10^{-8} Torr for different periods of time. Titration experiments were initiated 50 s after the oxygen supply had been turned off. The deuterium pressure used was 3.8×10^{-9} Torr (corresponding to a molecular flux of 3.8×10^{12} cm^{-2} s^{-1}) and the CO pressure 5.0×10^{-9} Torr (corresponding to a molecular flux of 1.9×10^{12} cm^{-2} s^{-1}). During the oxidation reactions, the D_2O or CO_2 background partial pressure in the chamber increased. These backgrounds have been subtracted from the mass spectrometer signals. In the case of D_2O, the background contribution was modeled by a curve fitting to the increase in the D_2O signal obtained by exposing the sample to D_2 without a previous exposure to oxygen. In the case of CO_2 desorption, two background effects were accounted for. First, the CO_2 increase which occurred when CO was introduced in the chamber, without a previous exposure to oxygen, was subtracted. Furthermore, the oxygen exposure that preceded the oxidation experiment introduced a drift in the CO_2 signal. This drift was also subtracted.

Deuterium has been used instead of hydrogen to study the water-forming reaction in order to avoid interference with the background of H_2O which is produced in the chamber during the oxygen pre-exposure of the sample. Note that we use the terms “water” and “hydrogen” irrespective of isotopic composition.

The sensitivity of the mass spectrometer used to record the desorption signals was regularly checked by backfilling the chamber with 0.35×10^{-9} and 1.4×10^{-9} Torr of Ar while registering the $m/e = 20$ and 40 signals.

3. Results and discussion

The oxidation experiments were always performed on a surface precovered with oxygen. The pre-exposures varied between 0.2 and 115 L. In view of what is known of oxygen adsorption on Pd(100) [5,6,9] we expect the p(2×2) phase to dominate the surface for the smaller oxygen exposures, but we also expect the presence of the more dense c(2×2) phase for the larger oxygen pre-exposures.

3.1. Carbon dioxide

Figure 1(a) shows the CO_2 desorption rates during CO exposures after different oxygen pre-exposures of the Pd(100) film. The sample temperature was kept at 300 °C. For pre-exposures up to 2.3 L the produced desorption rate is seen to be constant. For larger pre-exposures there is a tendency towards a slightly lower initial rate before the desorption rate reaches the constant maximum level. Independent measurements at this temperature also show that the desorption rate is directly proportional to the CO pressure.

Adsorbed oxygen does apparently not block or hinder the CO_2 formation whatsoever. The carbon dioxide desorption rate is, in principle, independent of θ_O, for $\theta_O > 0.02$.

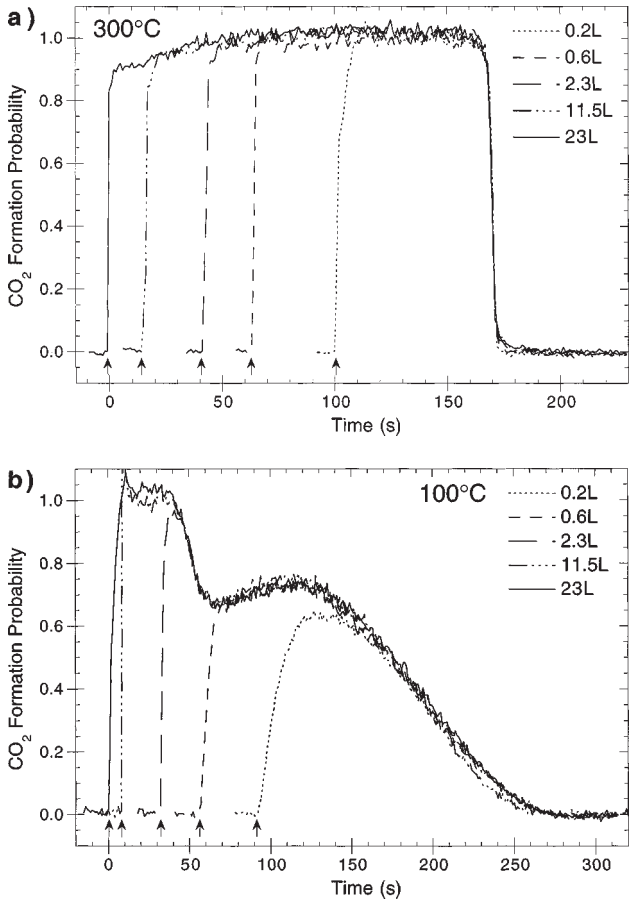

Figure 1. Time dependence of the CO_2 formation probability after different oxygen pre-exposures. The arrows mark where the CO flow is turned on. The sample temperature was (a) 300 and (b) 100 °C.

A similar behavior was also reported by Ertl et al. [12] for the CO_2 desorption rate from a Pd(111) surface for oxygen coverages between 0.08 and 0.25. At 300 °C and at the used CO pressure, the created CO coverage will always be very small (<0.02). Therefore, it is reasonable to fit the experimental data, as has been done in figure 1(a), to a very simple model assuming that the reactivity of all incoming CO molecules is equal to unity during the constant maximum CO_2 desorption rate level. Taking into account the CO flux and the time needed to consume the oxygen adsorbed during a certain oxygen pre-exposure, the amount of oxygen initially present can easily be calculated. The amount of pre-adsorbed oxygen desorbing as CO_2 for the 2.3 L exposure was determined and this result was used to calculate all other initial oxygen coverages by comparing the different integrated desorption rates of CO_2.

The CO_2 desorption results are compatible with a Langmuir–Hinshelwood reaction mechanism, assuming that CO adsorbs in a precursor state and displays a high surface mobility. It should be noted that it is possible and reasonable to describe the constant reaction rate as a product of θ_O and θ_{CO}, with published values of heats of adsorption for CO and O as input parameters. This results in an activation barrier for CO_2 formation, ΔE_{CO} of around 1 eV [21].

The CO_2 desorption rate is not greatly affected when the substrate temperature is reduced to 200 °C. At 100 °C, however, the desorption appearance changes drastically. The CO_2 formation rates at 100 °C, for different initial oxygen coverages, are plotted in figure 1(b). For large oxygen coverages (corresponding to $\theta_O > 0.18$, see figure 4) the initial desorption probability is equal to one, and independent of oxygen coverage. However, for smaller oxygen coverages the desorption rate is reduced. Furthermore, the on-set is fast for the larger initial coverages and the time to reach the equilibrium production rate is equal to the time it took to reach the desired CO pressure. This clearly implies that no substantial CO coverage is being formed during this stage. For the smaller oxygen coverages, the CO_2 desorption rate increases more slowly than the CO partial pressure does, suggesting that a CO coverage is built up before the equilibrium rate is obtained. This is especially obvious for the smallest initial oxygen coverage presented in figure 1(b), where a larger CO coverage has to be formed before equilibrium conditions are reached. During a subsequent oxygen exposure, CO_2 is produced and verifies that CO has been adsorbed.

We interpret the observed behavior in the following way. For the larger oxygen pre-exposures both the p(2 × 2) and the c(2 × 2) phases may be produced [5]. When CO is admitted, the c(2 × 2) phase is reduced first due to a higher reaction probability. Since the reactivity is close to unity, no CO is available for adsorption, and no substantial CO coverage is built up during this time. During the subsequent reduction of the less reactive p(2 × 2) phase, CO may adsorb, and this will in turn affect the further CO adsorption.

The rationale for the described interpretation is the following. The heat of adsorption for the c(2×2) oxygen phase is distinctly lower than that of the p(2×2) phase [5,6]. Thus, by applying the theory of bond-order conservation [22,23] it can be seen that also the heat of CO_2 formation, ΔE_{CO_2}, will decrease, resulting in an increase of the CO_2 formation rate for the c(2 × 2) phase. Since these changes are very directly connected to the existence of the c(2 × 2) phase, it is expected that the rate should decrease rapidly when this phase has been consumed.

3.2. Water

Figure 2 shows the water formation probabilities while exposing the Pd(100) film, precovered with different amounts of oxygen, to D_2 at 300 °C. In contrast to the carbon dioxide production at 200 and 300 °C, the water formation rate is obviously strongly affected by the pre-adsorbed oxygen. The formation rate grows as the oxygen coverage is reduced and reaches a maximum when the oxygen coverage is very small. When all oxygen has been removed the water desorption rate drops abruptly.

The calibration of the ordinate in figure 2 has been made following the assumption from figure 1(a), by also assuming that the same amount of oxygen leaves the surface as D_2O as would leave the surface as CO_2 (one pre-adsorbed

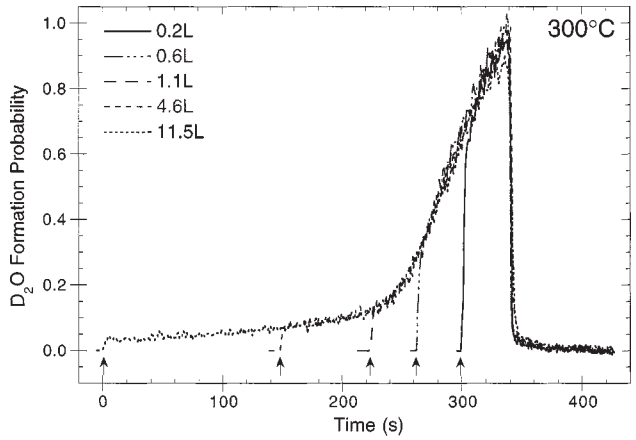

Figure 2. Time dependence of the D_2O formation probability after different oxygen pre-exposures. The arrows mark where the D_2 flow is turned on. The sample was kept at 300 °C.

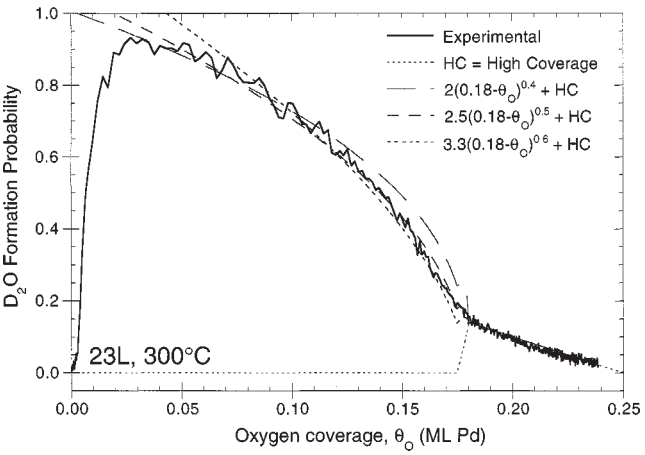

Figure 3. The D_2O formation probability as a function of oxygen coverage at 300 °C. The dashed lines show some attempts for theoretical modeling.

oxygen atom per desorbing CO_2 molecule) for the same oxygen pre-exposure.

The D_2O formation rate is obviously a single-valued function of the oxygen coverage, at least as long as the oxygen pre-exposures are smaller than 23 L (discussed below). Thus, regardless of oxygen pre-exposure the desorption rate at a certain oxygen coverage is always the same. In figure 3 the formation rate is presented as a function of oxygen coverage instead of time. (The oxygen coverage is determined from the initial oxygen coverage minus that consumed by the reaction.) From this plot it is clear that the water desorption cut-off occurs when the oxygen coverage is less than 0.02, i.e., the water formation maximum appears when the oxygen coverage is as low as 0.02–0.03! It is further interesting to note that there is an apparent change in formation probability at an oxygen coverage of approximately 0.18. We have previously shown that for polycrystalline Pd surfaces the water-forming rate is proportional to $(\alpha - \theta_O)^x$ with $x = 1$ and $\alpha = 0.25$ [17] for oxygen coverages above the rate maximum. This rate simply mirrors the oxygen blocking ability of the H_2 dissociation. From figure 3 a linear behavior seems reasonable for $\theta_O > 0.18$, but for lower oxygen coverages x seems to be smaller than 1. On the other hand, α also changes and becomes smaller than 0.25, giving a fairly complicated behavior of the hydrogen dissociation rate with oxygen coverage.

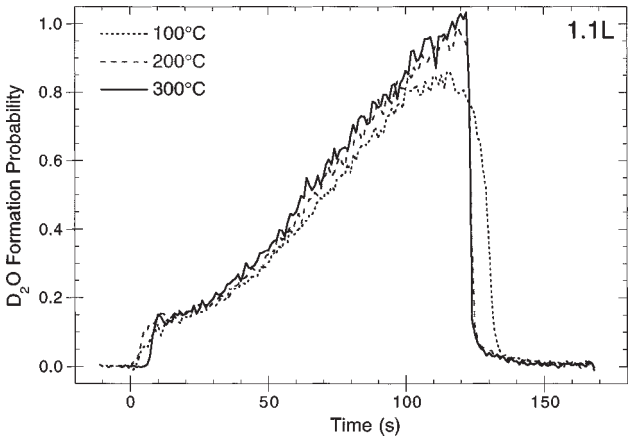

Figure 4. Time dependence of the D_2O formation probability after a 1.1 L oxygen pre-exposure, for different sample temperatures.

The long "induction period" in the water formation viewed for coverages above $\theta_O = 0.18$ on the Pd(100) film (c.f. figure 2) has not been observed for Pd(111) and (110) [1]. Nor has this change in oxygen dependence been reported by, e.g., Fogelberg et al. [17], who have performed titration experiments on dense Pd films grown on SiO_2.

Again, the reaction behavior can be interpreted as a consequence of oxygen being adsorbed in different phases. As discussed in section 1 it is reasonable to assume that for larger coverages than $\theta_O = 0.18$, the c(2 × 2) oxygen phase is formed alongside the p(2 × 2) phase. Both of these phases block hydrogen adsorption/dissociation effectively. In view of the low oxygen density on the p(2 × 2) phase, this really demonstrates a "long-range" efficiency of the oxygen blockage. The oxygen-free surface area (available for hydrogen adsorption) will, furthermore, not grow significantly if the hydrogen that does adsorb for geometrical reasons primarily reacts with the dense c(2 × 2) oxygen, reducing the c(2 × 2) phase to a less dense phase, which may continue to block hydrogen adsorption. In accordance with the findings presented by Simmons et al. [5] we suggest that there is a sequential reduction of the oxygen phases. First, the more dense c(2 × 2) phase is slowly reduced to a p(2 × 2) phase, not causing any significant increase in surface area available for hydrogen dissociation. This is followed by a more rapid reduction of the p(2 × 2) phase, during which there is a continuous increase of the surface area for hydrogen adsorption and dissociation. At this stage the water reaction accelerates.

The temperature dependence of the water-reaction process is rather small. The overall behavior does stay the same, see figure 4, even though the cut-off is less sharp and there is a slight reduction in the maximum rate at 100 °C as compared to 300 °C. The process remains a single-valued function of oxygen (for pre-exposures less than 23 L),

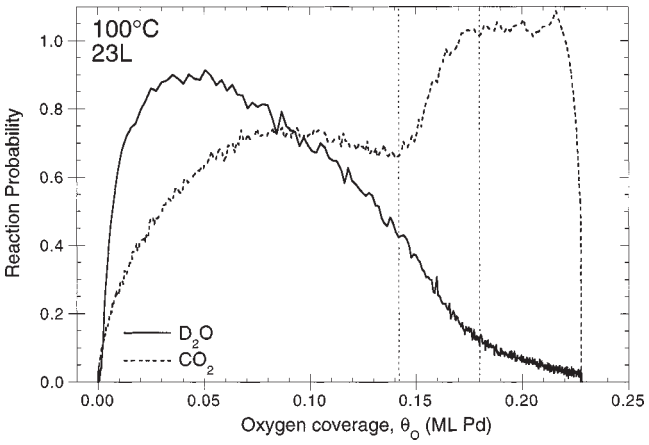

Figure 5. The formation probabilities for D_2O and CO_2 as a function of oxygen coverage, after 23 L oxygen at 100 °C.

demonstrating also the same change in oxygen dependency at around $\theta_O = 0.18$. The less sharp cut-off and the reduction in maximum rate have also been observed on dense polycrystalline Pd films grown on SiO_2, as the substrate temperature was reduced. In fact, the reaction kinetics for that system have been successfully modeled and the temperature effect is well accounted for [16,17]. The reduced maximum rate and the slower cut-off is simply an effect of the reduction in the rate of hydroxyl formation [18], also giving rise to a slight increase in the hydrogen coverage with decreasing temperature.

In figure 5, the water and the carbon dioxide desorption rates have been plotted as a function of oxygen coverage, for a 23 L pre-exposure of oxygen and at a substrate temperature of 100 °C. The difference in functional behavior is obvious. Whereas the desorption rate for water is very small at higher coverages, the carbon dioxide desorption is unaffected by the adsorbed oxygen. Even though the changes in the desorption rates at $\theta_O = 0.18$ are the opposite, the coincidence is clear and supports the interpretation that the desorption rate changes are related to the state of the oxygen coverage.

3.3. Oxygen adsorption isotherm

In figure 6(a), the initial oxygen coverage is plotted vs. oxygen exposure for a series of measurements performed at 300 °C. Also shown is the theoretical adsorption isotherm calculated assuming that the adsorption rate is proportional to $(0.23 - \theta_O)^2$ and that the initial sticking coefficient is equal to one. The oxygen saturation coverage of 0.23 ML (monolayers) of Pd(100) was determined by fitting the theoretical adsorption isotherm to the oxygen coverage produced by a 11.5 L exposure. It should be noted that the saturation coverage, expected for the p(2 × 2) phase alone, is 0.25 and probably the accuracy of our measurement is not better than that the determined coverage of 0.23 could actually be 0.25. In figure 6(b), the same type of results as in figure 6(a), oxygen coverage vs. exposure, is plotted together with an adsorption isotherm, for 100 °C. At

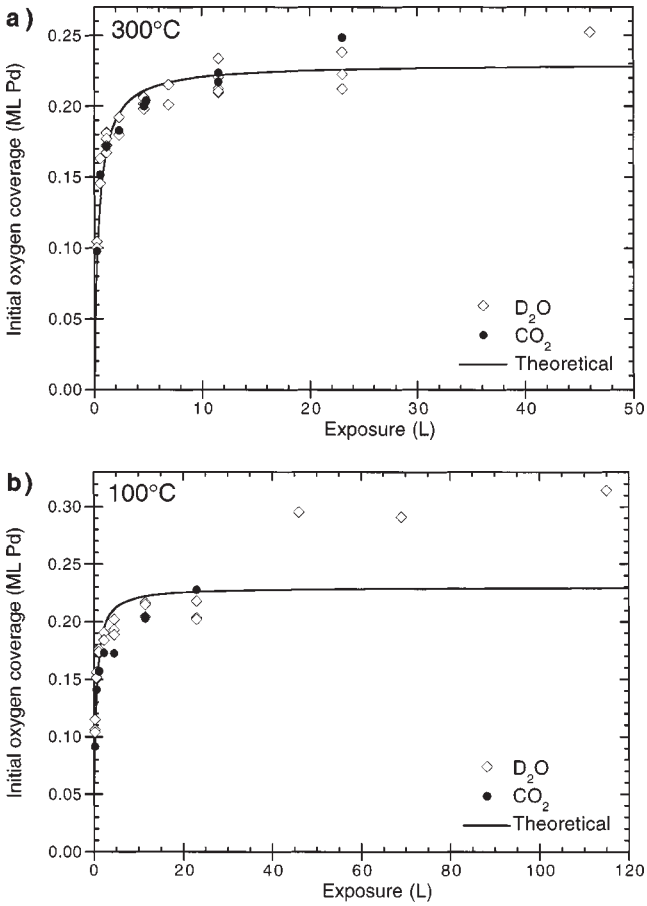

Figure 6. Initial surface coverage as a function of oxygen pre-exposure for a sample temperature of (a) 300 and (b) 100 °C. The solid line is calculated assuming an oxygen rate of adsorption dependent on $S^0_{O_2}(0.23-\theta_O)^2$ with $S^0_{O_2} = 1$.

300 °C the experimental results initially follow the isotherm quite well, perhaps with a deviation for the largest exposure. At 100 °C there is clearly a discrepancy between the theoretical curve and the experimental results at larger exposures. For the larger exposures the oxygen coverage exceeds the "saturation coverage", again suggesting the presence of a second more closely packed oxygen structural phase.

The water desorption rates presented so far have all been produced after oxygen pre-exposure of less than 23 L and it has been obvious that eventually the rates all follow the same desorption rate curve no matter what the initial coverage (cf. figure 2). If the pre-exposure exceeds 23 L this will, however, no longer be the case, see figure 7 (a) and (b). For larger oxygen exposures the desorption-rate maximum will be reduced and the cut-off will become less sharp. The effect is amplified for increasing exposures.

This we believe reflects a situation where the p(2 × 2) phase is gradually and slowly replaced by the c(2 × 2) phase. Consequently the reduction in the water formation rate maximum can be understood provided the high oxygen density c(2 × 2) phase increases the hydroxyl formation energy barrier, ΔE_{OH}. An alternative explanation would

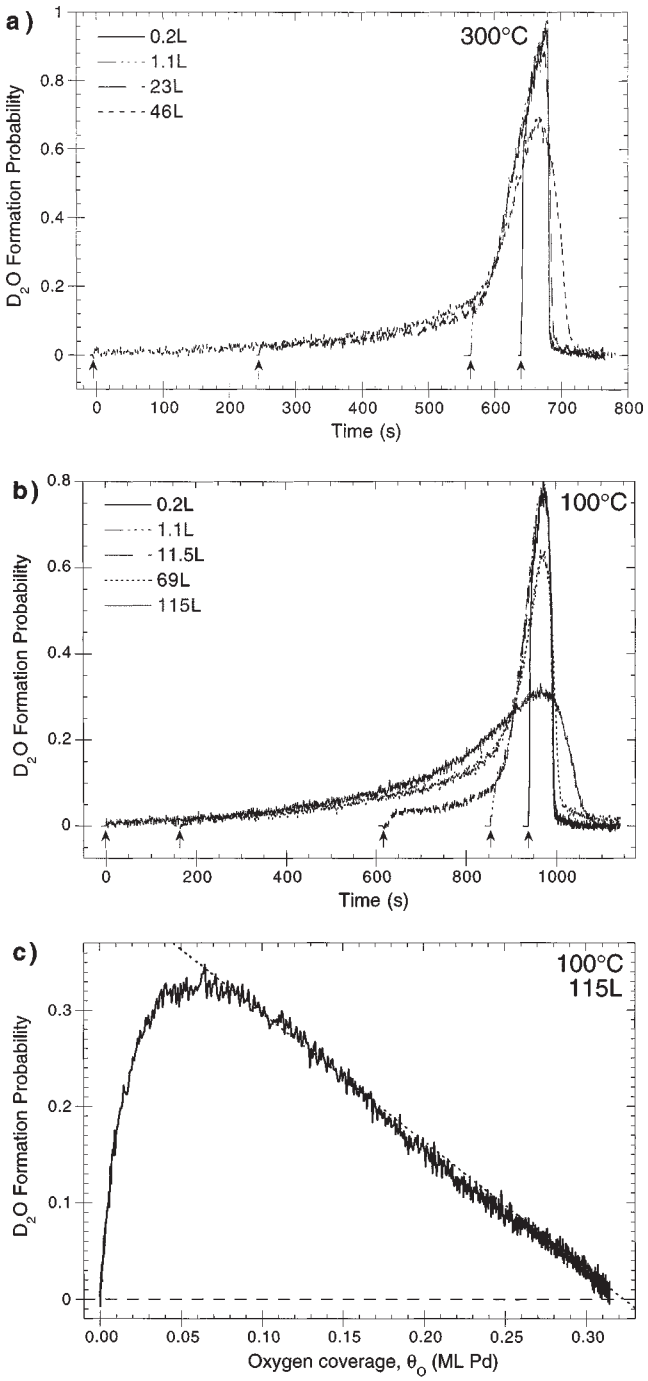

Figure 7. D_2O formation probability as a function of time for different oxygen pre-exposures (including exposures greater than 23 L), at (a) 300 and (b) 100 °C. In figure (c) the D_2O formation probability is presented as a function of oxygen coverage, at 100 °C.

be that oxygen islands are formed, allowing only boundary oxygen to react.

It is interesting to note that the water desorption rate, plotted as a function of oxygen coverage for an oxygen pre-exposure of 115 L, shown in figure 7(c), displays a linear dependence. This is in agreement with the discussion in connection with figure 3, where the linear part of the desorption rate was coupled to the reduction of the c(2 × 2) phase.

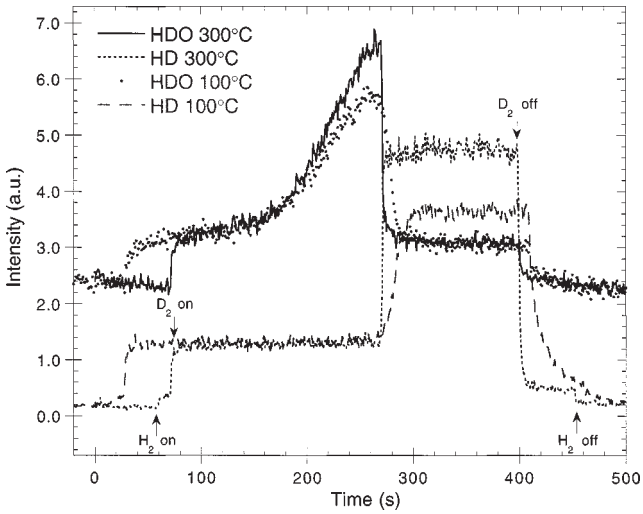

Figure 8. The HD and HDO mass spectrometer signals during combined H_2 (flux: 1.6×10^{16} molec./m^2) and D_2 (flux: 1.9×10^{16} molec./m^2) exposures after a 4.6 L oxygen pre-exposure. Note that no background subtractions have been made in the figure, i.e., the steps seen in the signals, when H_2 and D_2 are turned on and off, are due to the background and are not related to the sample.

3.4. D_2 and H_2 mixed

In figure 8, the HDO and HD formation from an oxygen-precovered Pd(100) film exposed to equal fluxes of H_2 and D_2 is shown, for two different film temperatures, 100 and 300 °C. Note that the HD production does not start until the water formation has reached its cut-off. The interpretation must be that all available hydrogen/deuterium atoms on the surface, as long as there is oxygen present, form water and desorb prior to associating and desorbing as H_2, D_2 or HD. Thus, oxygen will block hydrogen adsorption and dissociation, but once hydrogen has dissociated on the surface, the water-forming reaction is extremely effective and will consume all hydrogen/deuterium. The water formation rate is therefore a true measure of the hydrogen sticking coefficient. At 300 °C, the coincident HDO cut-off and the HD on-set are very quick. At 100 °C the switch is slower reflecting a build-up of a (small) hydrogen coverage. Furthermore, at 100 °C the HD steady-state level is lower than at 300 °C, indicating a larger steady-state hydrogen coverage on the surface at the lower temperature.

4. Summary and conclusions

The water and carbon dioxide desorption rates vs. time or oxygen coverage show very different functional behaviors. While adsorbed oxygen on the Pd(100) surface shows a very effective blocking for hydrogen adsorption and dissociation; CO adsorption is almost unaffected. At temperatures above 200 °C, the reactivity of CO is almost independent of oxygen coverage and assumed to be equal to one, while for an oxygen pre-coverage greater than 0.18, the hydrogen reaction probability is very low. The hydrogen

reactivity reaches its maximum when the oxygen coverage has been reduced and is very low, $\theta_O < 0.03$.

Both the CO_2 desorption rate, at 100 °C, and the water desorption rate, at all temperatures studied, show a change in reaction behavior at an oxygen coverage of approximately 0.18. We would like to attribute this change to the sequential reduction of oxygen adsorbed in different phases on the Pd(100) surface. We propose the following:

(i) For small oxygen coverages ($\theta_O < 0.18$) only the p(2 × 2) phase is formed, with an initial sticking coefficient equal to one. This phase is readily reduced by CO at temperatures ⩾200 °C, while at 100 °C, the oxidation efficiency is reduced, partly as a consequence of a decrease in the reaction constant and partly as a consequence of increased CO adsorption. Hydrogen is effectively blocked even by the low-density p(2 × 2) oxygen, but once hydrogen dissociation is possible, the water reaction accelerates quickly.

(ii) For somewhat larger oxygen coverages, $0.18 < \theta_O < 0.23$, a small portion of c(2 × 2) phase oxygen is formed alongside the almost saturated p(2 × 2) phase. This surface is very resistant to hydrogen adsorption. The small amount of hydrogen that does adsorb primarily reduces the c(2 × 2) oxygen, and even though some water is formed, the surface area for hydrogen adsorption is not significantly increased, whence the long induction period. The water formation turns to a p(2 × 2) behavior when the c(2 × 2) phase has been consumed. For CO, at sample temperatures above 200 °C, both oxygen phases are consumed with unity efficiency. When the temperature is reduced to 100 °C, however, the c(2 × 2) oxygen, with a smaller heat of adsorption than the p(2 × 2) oxygen, is reduced first, with a reactivity of one and with no evidence for contemporary CO adsorption. During the subsequent reduction of the p(2 × 2) phase, the CO coverage will start to grow.

(iii) Finally, for pre-exposures ⩾23 L ($\theta_O = 0.23$) we believe that the p(2×2) phase gradually is replaced by, or transformed to, the c(2 × 2) phase. This has an effect on the water formation either due to an increase in the hydroxyl formation barrier (this is the rate-limiting activation energy in the water-forming reaction [16,17]) or due to a c(2 × 2) island formation, where hydrogen only can react with oxygen atoms at the perimeter of the islands.

Acknowledgement

We thank Dr. Mats Eriksson for fruitful discussions and ideas concerning this work, which was financed by the Swedish Foundation for Strategic Research (SSF) through the Materials Research Consortium on Thin Film Growth, and by the Swedish National Science Research Council (NFR).

References

[1] H. Fornander, H. Dannetun and L.-G. Ekedahl, in manuscript.
[2] H. Fornander, H. Dannetun and L.-G. Ekedahl, in manuscript.
[3] H. Fornander, L. Hultman, J. Birch and J.-E. Sundgren, J. Cryst. Growth 186 (1998) 189.
[4] H. Fornander, J. Birch, L. Hultman, L.-G. Petersson and J.-E. Sundgren, Appl. Phys. Lett. 68 (1996) 2636.
[5] G.W. Simmons, Y.-N. Wang, J. Marcos and K. Klier, J. Chem. Phys. 95 (1991) 4522.
[6] S.-L. Chang and P.A. Thiel, J. Chem. Phys. 88 (1988) 2071.
[7] T.W. Orent and S.D. Bader, Surf. Sci. 115 (1982) 323.
[8] G. Ertl and J. Koch, in: *Proc. 5th Int. Congr. on Catalysis*, ed. J. Hightower (North-Holland, Amsterdam, 1973) p. 969.
[9] E.M. Stuve, R.J. Madix and C.R. Brundle, Surf. Sci. 146 (1984) 155.
[10] N.C. Bartelt, L.D. Roelofs and T.L. Einstein, Surf. Sci. Lett. 221 (1989) 750.
[11] G. Ertl and J. Koch, Z. Phys. Chem. 69 (1970) 323.
[12] T. Engel and G. Ertl, J. Chem. Phys. 69 (1978) 1267.
[13] H. Conrad, G. Ertl and J. Küppers, Surf. Sci. 76 (1978) 323.
[14] J. Goschnick, J. Loboda-Cackovic, J.H. Block and M. Grunze, in: *Kinetics of Interface Reactions*, Vol. 8, eds. M. Grunge and H.J. Kreuzer (Springer, Berlin, 1987) p. 269.
[15] L.-G. Petersson, H.M. Dannetun and I. Lundström, Surf. Sci. 161 (1985) 77.
[16] M. Eriksson, Ph.D. thesis, Linköping University, Sweden (1997).
[17] J. Fogelberg, Ph.D. thesis, Linköping University, Sweden (1994).
[18] J. Fogelberg and L.-G. Petersson, Surf. Sci. 350 (1996) 91.
[19] F. Nakao, Vacuum 25 (1975) 431.
[20] H. Dannetun, Ph.D. thesis, Linköping University, Sweden (1987).
[21] M. Eriksson and L.-G. Ekedahl, Surf. Sci. 412/413 (1998) 430.
[22] E. Schustorovich, Surf. Sci. Lett. 176 (1986) 863.
[23] E. Schustorovich, Surf. Sci. Lett. 187 (1987) 627.